Low-Energy Measurement of the ^{7}Be$(p,\gamma)^8$B Cross Section

F. Hammache,[1,*] G. Bogaert,[1,†] P. Aguer,[2] C. Angulo,[3] S. Barhoumi,[5] L. Brillard,[4] J. F. Chemin,[2] G. Claverie,[2] A. Coc,[1] M. Hussonnois,[4] M. Jacotin,[1] J. Kiener,[1] A. Lefebvre,[1] C. Le Naour,[4] S. Ouichaoui,[5] J. N. Scheurer,[2] V. Tatischeff,[1] J. P. Thibaud,[1] and E. Virassamynaïken[2]

[1]*CSNSM, IN2P3-CNRS, F-91405 Orsay et Université de Paris-Sud, France*
[2]*CENBG, IN2P3-CNRS, et Université de Bordeaux I, F-33175 Gradignan, France*
[3]*Centre de Recherches du Cyclotron, UCL, Chemin du Cyclotron 2, B-1348 Louvain la Neuve, Belgium*
[4]*IPN, IN2P3-CNRS et Université de Paris-Sud, F-91406 Orsay, France*
[5]*Institut de Physique, USTHB, B.P. 32, El-Alia, Bab Ezzouar, Algiers, Algeria*

(Received 23 May 2000)

We have measured the cross section of the ^{7}Be$(p,\gamma)^8$B reaction for $E_{\text{c.m.}} = 185.8$, 134.7, and 111.7 keV using a radioactive ^{7}Be target (132 mCi). Single and coincidence spectra of β^+ and α particles from ^{8}B and ^{8}Be* decay, respectively, were measured using a large acceptance spectrometer. The zero energy S factor inferred from these data is 18.5 ± 2.4 eV b and a weighted mean value of 18.8 ± 1.7 eV b (theoretical uncertainty included) is deduced when combining this value with our previous results at higher energies.

DOI: 10.1103/PhysRevLett.86.3985 PACS numbers: 25.40.Lw, 21.10.Pc, 26.65.+t, 27.20.+n

Recent experimental results on solar ν_e and atmospheric ν_μ neutrinos support neutrino oscillation scenarios, in which the oscillation probability depends on the neutrino mixing angles and squared mass differences. For ν_e-ν_x oscillation, the determination of these fundamental quantities needs accurate solar modeling and nuclear cross sections for the reactions operating in the solar core [1–3]. In this respect, the most important nuclear physics parameter is the S factor of the ^{7}Be$(p,\gamma)^8$B reaction which gives rise to the crucial ^{8}B neutrinos [4]. In a previous work [5], we have measured the ^{7}Be$(p,\gamma)^8$B reaction cross section for $E_{\text{c.m.}} = 0.35$–1.4 MeV using radioactive ^{7}Be targets. In this Letter, we report on new direct measurements of this cross section at center of mass energies below 200 keV, where extrapolation to solar energies ($E_{\text{c.m.}} = 18$ keV) is expected to be almost free of theoretical uncertainties [6], which is not the case for measurements at higher energies.

The electrostatic accelerator PAPAP at Orsay supplied intense proton beams of well-calibrated energies [7]. We used a highly radioactive ^{7}Be target (131.7 mCi) prepared as in Refs. [8,9] additionally containing approximately 3×10^{16} atoms of ^{9}Be. β^+ and α particles from $^8\text{B}(\beta^+)^8\text{Be}^*(2\alpha)$ decays were detected at forward and backward angles, respectively. We used the solenoidal superconducting magnet SOLENO [10] (3.2 T at the center, 1.22 m long, 32 cm of internal diameter) in order to detect both α and β^+ particles with high efficiency (11.5% and 25%, respectively) due to the focusing power of the field. Both singles and coincidence events between α and β^+ particles were recorded, the latter providing spectra free of background events even at low bombarding energies.

Off-beam detection (^{8}B period = 0.77 s) was necessary to avoid any contamination in both α and β^+ coincidence spectra arising from the channel ^{7}Li$(p,\gamma_1)^8$Be$^*(2\alpha)$. In this reaction the α decay of ^{8}Be* is the same as in $^8\text{B}(\beta^+)^8\text{Be}^*(2\alpha)$ and the β^+ detector could not efficiently discriminate β^+ particles of interest from electron pairs produced in the target assembly by γ_1 rays ($E_{\gamma 1} = 14.8$ MeV).

For the delayed detection purpose, the beam passed through an electrostatic deflector which was alternately switched on and off for time periods of 1.5 s. The prompt events from ^{9}Be$(p,\alpha)^6$Li and ^{9}Be$(p,d)^8$Be were also recorded and used later for energy calibration of the α detectors and normalization purpose (see below).

The target was located near the solenoid center, perpendicular to the symmetry axis of the field. The target backing of 0.1 mm ultrapure platinum and its holder allowed both efficient water cooling and large transmission for β^+ particles. The beam spot at the target position was made visible by using an alumina (Al_2O_3) target which could be moved to the exact position of the target. An optical system provided a magnified image of the beam spot to measure its position and size on the target. They were systematically determined (size about 10 mm^2) before and after each run.

In order to prevent carbon buildup on the target, a copper plate cooled with liquid nitrogen was placed in the target vicinity. In addition, cryogenic, turbomolecular, and ionic pumps were used to keep the vacuum below 5×10^{-7} mbar during the whole experiment.

Typical beam currents of 10–40 μA on the target were used. To suppress secondary electron escape, the target was biased at a positive 300 V. As a consistency check, currents were also measured in the insulated chamber where the beam was periodically deflected, at the SOLENO entrance collimator and at the α detector tube (see below) where negligible currents were observed. All the currents were integrated, digitized, recorded cycle-by-cycle, and analyzed off-line. Very good agreement was found between integrated charges for beam on target and

beam off target, and the overall uncertainty on the target integrated charge was 2%.

β^+ particles ($E_{max} = 14$ MeV) were detected in a set of 6 successive cylindrical plastic scintillators (diameter 20 mm and thickness 3, 3, 8, 8, 8, and 10 mm) centered on the field axis and 22 cm away from the target. The number and thickness of the plastic scintillators were optimized from GEANT simulations [11] to discriminate MeV β^+ particles from the huge number of γ rays and photoelectrons produced in the target backing by the $E_\gamma = 478$ keV radiation from ^{7}Be decay while still measuring β^+ energies with a reasonable precision. This discrimination was effective when at least two β detectors were required to fire.

α particles (from ^{8}Be* decay) with energies below 3.5 MeV and emission angles between approximately 95° and 150° with respect to the beam direction were deflected towards the solenoid axis and detected in an array of 6×4 Si detectors (22 mm $\times$ 45 mm $\times$ 0.1 mm). The detectors were mounted in cylindrical geometry (internal diameter of 4 cm) aligned on the solenoid axis. Depending on energy and emission angle, α particles were detected at distances ranging from 18 to 36.5 cm from the target. Backscattered protons were deflected along different paths and were not able to reach the α detectors.

The data were recorded event by event. They included the measurements of α and β^+ energies, number and identification of detectors fired, and the time of flight difference between α and β^+ particles for coincidence events. In the data analysis, events where more than one α detector or less than two β^+ detectors fired were rejected. A pulse generator was used for dead time measurements.

Cross section measurements were performed at three proton energies, 217 keV, 160 keV, and 130 keV. The absolute value of the cross section at the proton energy of 217 keV was obtained counting singles delayed α particles in the range from 1 to 3.36 MeV. Figure 1(a) shows the corresponding spectrum, obtained by adding together the individual α spectra measured in the silicon detectors.

The calibration of the silicon detectors was performed using the three well-defined peaks observed in the singles prompt spectra from ^{9}Be$(p,d)^8$Be and ^{9}Be$(p,\alpha)^6$Li reactions. Data shown in Fig. 1(a) were obtained after subtraction of the background contribution which was determined in a series of measurements of several days with the beam off and the active target in place. A check was made to ensure that a null extra background (within statistical uncertainties) was introduced when the beam hit a pure platinum target. Background subtraction was performed by simply normalizing the corresponding spectrum to counting time. For comparison, the coincidence delayed α particle spectrum measured in the same runs is shown in Fig. 1(b). It can be seen in Fig. 1 that the low energy (<1 MeV) component in the singles spectrum, corresponding to pileup events due to photoelectrons created by the 478 keV γ rays, has completely vanished in the coincidence spectrum. The solid curve in Fig. 1(b) is obtained from a least squares fit to this background free coincidence spectrum. We see in Fig. 1(a) that the same curve also provides a reasonable fit to singles data (after normalization to counting), as expected from an unbiased background subtraction process.

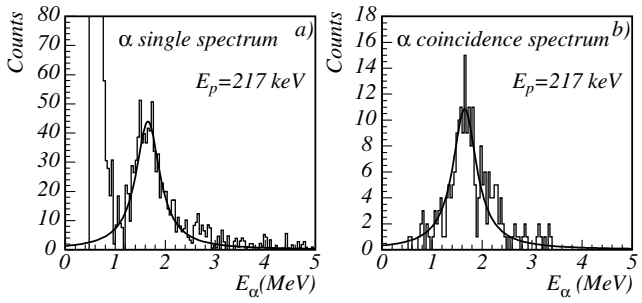

FIG. 1. (a) Energy spectrum of singles delayed α particles. (b) Energy spectrum of delayed α particles detected in coincidence with delayed β particles.

The α detection efficiency in the 1.00–3.36 MeV energy range was determined with the same detection setup from an analysis of the reaction ^{7}Li$(p,\gamma_1)^8$Be* performed with an enriched ^{7}Li target at $E_p = 160$ keV. As explained above, the 14.8 MeV γ_1 rays create e^+-e^- pairs in the target backing which were detected in the plastic scintillator counter, while ^{8}Be* decay into two α particles detected in the silicon array [the same α's as in the channel ^{8}B$(\beta^+)^8$Be*]. The α detection efficiency was deduced from the number of counts in the plastic scintillator taken in singles and in coincidence with the silicon detector. The singles γ_1 ray yield was taken to be 0.680 ± 0.043 [12] times the total counts arising in the plastic scintillator from both γ_0 and γ_1 channels. GEANT simulations confirmed that pair detection efficiencies were the same, within less than 1%, for γ_0 and γ_1. The angular correlation between e^+-e^- pairs and α particles was also calculated and found negligible for the s-wave proton capture at this low bombarding energy.

A kinematics correction of 9.6% was applied to the experimental efficiency value to take into account the ^{8}Be* in flight decay in the ^{7}Li$(p,\gamma_1)^8$Be* reaction. Finally, the detection efficiency was $\epsilon_\alpha = 0.115 \pm 0.008$ in the 1.00–3.36 MeV energy range, in fair agreement with GEANT simulations (12%).

The ^{7}Be total activity at the beginning and at the end of the run at 217 keV, the target area (0.47 ± 0.02 cm^2) and the ^{7}Be activity profile were accurately determined with the same instruments and methods used in the experiment described in Ref. [5]. After fitting the ^{7}Be decay function to the measurements, we found an initial total activity of 131.7 ± 2.4 mCi. No loss of activity due to beam impact was observed during the run. The ^{7}Be areal density over the beam spot was finally determined run by run (9% uncertainty) by averaging the results of the 478 keV γ ray scan over the beam spot dimensions and normalizing them to the total activity per unit surface area.

A value of $\sigma = 16.7 \pm 2.1$ nb at the incident proton energy of 217 keV was deduced [see the formula (3) in

Ref. [13]]. This value takes into account a 1% correction due to the ^{8}B backscattering on platinum atoms and escape out of the target [14]. This correction was calculated using a TRIM [15] simulation with target thickness and composition determined from consistent Rutherford backscattering spectrometry (RBS), (d, p), and proton-induced x-ray emission spectrometry (PIXE) analysis measurements performed during the course of the experiment. At the beginning of the experiment, the target was found to contain mainly carbon (9 μg/cm^2), oxygen (7.6 μg/cm^2), and less than 4 μg/cm^2 of calcium and other lighter elements, corresponding to a thickness of 9.6 $\pm$ 1.0 keV for protons of 217 keV.

This thickness leads to an effective energy of 212.4 keV ($E_{\text{c.m.}} = 185.8$ keV) and an S factor value of 17.2 $\pm$ 2.1 eV b. The quoted uncertainty includes the 6.3% uncertainty in the γ_1 branching ratio [12] of ^{7}Li$(p, \gamma)^8$Be*.

The cross sections at $E_p = 130$ and 160 keV were determined using α-β coincidence measurements only, because of the decrease of the signal over background ratio observed in singles spectra with lowering bombarding energies. The corresponding coincidence α energy spectra are shown in Fig. 2 together with time difference spectra between α and β^+ particles. The 3 peaks in the time spectra correspond to 3 classes of trajectories where α particles can spiral 1, 2, or 3 times in the magnetic field before reaching the detectors. The rare counts found between the peaks and at $\Delta t = 200$ ns (i.e., null time of flight difference) in Fig. 2(b) are background events (most probably cosmic rays) eliminated in the energy spectra by gating on the three time peaks.

S factors at $E_p = 160$ keV and $E_p = 130$ keV, relative to the one measured at $E_p = 217$ keV, were obtained by normalization to the α yield from the reaction ^{9}Be$(p, \alpha)^6$Li through the relation

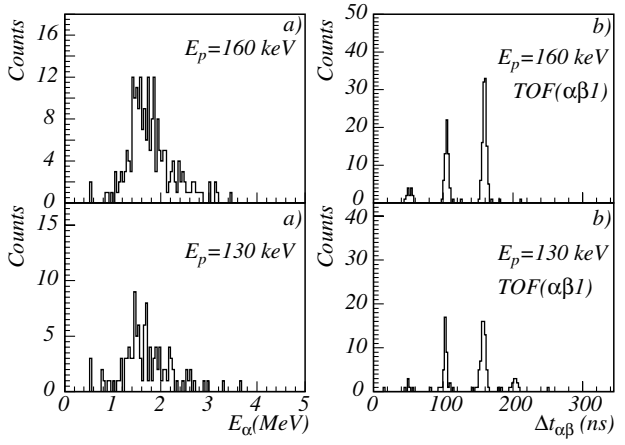

FIG. 2. (a) Energy spectra obtained at 160 and 130 keV for delayed α particles detected in coincidence with delayed β particles. (b) Corresponding spectra for time difference between α and β^+ particles obtained using the first of the six plastic scintillators. A null time of flight difference is arbitrarily at 200 ns due to delays in the electronics.

$$\frac{S^7(E^7_{\text{cm}_{2,3}})}{S^7(E^7_{\text{cm}_1})} = K\,\frac{R(E_{2,3})^{7,9}}{R(E_1)^{7,9}}\,\frac{S^9(E^9_{\text{cm}_{2,3}})}{S^9(E^9_{\text{cm}_1})}\,e^{-\lambda^{^7\text{Be}}(\Delta t_{1i})}, \quad (1)$$

where the subscripts 1, 2, and 3 label the runs at $E_p =$ 217 keV, 160 keV, and 130 keV, respectively, and the superscripts 7 and 9 label the reactions ^{7}Be$(p, \gamma)^8$B and ^{9}Be$(p, \alpha)^6$Li, respectively. $R(E_i)^{7,9}$ is the coincidence yield normalized to the α yield from the ^{9}Be$(p, \alpha)^6$Li reaction, S^9 is the astrophysical S factor of the ^{9}Be$(p, \alpha)^6$Li reaction at the corresponding c.m. effective energy. K is a constant accounting for the changes in dead times, in effective time parameters (see parameter β in formula 4 of Ref. [13]) and in angular distributions of alphas in ^{9}Be$(p, \alpha)^6$Li with the bombarding energies. These three corrections were found to be very small (less than a few percent). The exponential term, in which Δt_{1i} is the time difference between experiments i and 1, accounts for the decrease in the ^{7}Be target activity with time.

In calculating R, the α yield from ^{9}Be$(p, \alpha)^6$Li resulted from a least-squares analysis of the prompt singles spectra where very well-defined α peaks show up. S factors and angular distributions concerning the ^{9}Be$(p, \alpha)^6$Li reaction were taken from the literature [12].

It must be stressed that the normalization to the α yield from ^{9}Be$(p, \alpha)^6$Li eliminates effects due to target nonuniformity, beam position variation, and loss of activity of the target due to beam impact as long as the ratio of atomic densities of ^{9}Be to ^{7}Be remains constant. This is expected since ^{9}Be was introduced in the ^{7}Be solution before electrodeposition of the final target. It was verified experimentally through a comparison of ^{7}Be γ-ray scan with a ^{9}Be scan using (d, p) reaction analysis with a microbeam. A non-negligible loss of activity was actually observed after the runs at $E_p = 160$ and 130 keV, because of a significant increase of sputtering effects with decreasing energy.

For the calculations of the proton energy losses at 160 and 130 keV, we took into account the loss of target material by the monitoring of the ^{9}Be content through the ^{9}Be$(p, \alpha)^6$Li reaction. We estimated the uncertainty on the effective energy to be 2.5 keV, which induces an uncertainty of 2% on the ratio $S^9(E^9_{\text{c.m.}_{2,3}})/S^9(E^9_{\text{c.m.}_1})$.

Taking into account a 1% loss of ^{8}B nuclei due to the ^{8}B backscattering [14] we deduced the astrophysical S factor values of $S(134.7\text{ keV}) = 19.5 \pm 3.1$ eV b and $S(111.7\text{ keV}) = 15.8 \pm 2.7$ eV b. Final uncertainties were calculated by quadratic summation of all individual uncertainties related above.

Results for the astrophysical S factor are shown in Fig. 3. Extrapolation to zero energy using the calculations of Ref. [16] and the present low-energy data gives $S(0) = 18.5 \pm 2.4$ eV b where the error bar is only experimental. A negligible dispersion of $S(0)$ is found (0.2 eV b) when various calculated curves [16,17] of $S(E)$ are fitted to the same data. This reflects the agreement between models at low energy, since the interaction in that case takes place at very large ^{7}Be-p distances and is mainly governed by Coulomb physics. As a consequence

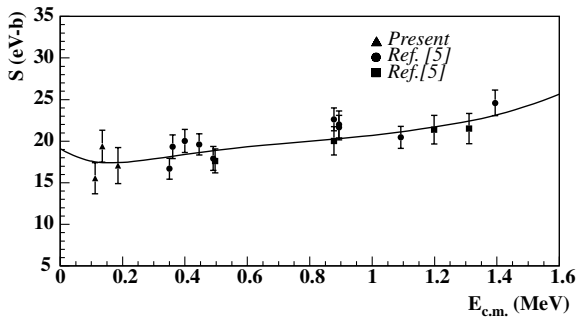

FIG. 3. Measured S factors from the present work and from Ref. [5] after backscattering correction [5]. Error bars represent random uncertainties. The curve through the data, given for illustrative purposes, is a fit to the three sets of data, assuming independent errors and using the calculation of Ref. [16].

the total uncertainty (experimental + theoretical) is finally ± 2.4 eV b.

Using the calculation of Ref. [16], our previous measurements [5] lead to $S(0) = 19.1 \pm 1.2$ eV b [18], where the error bar is experimental. As the experiment was performed at higher energies, sophisticated nuclear calculations are required in that case to describe the shape of $S(E)$ which leads to a higher theoretical uncertainty on $S(0)$. An $S(0)$ dispersion of ± 2 eV b was found using the available models [16,19] to fit the data. Adding this dispersion, considered as a reasonable estimate of the theoretical uncertainty, to the experimental error bar and combining quadratically the obtained result for $S(0)$ with that of the present low-energy result, we finally obtain a weighted mean value of $S(0) = 18.8 \pm 1.7$ eV b (taking a more conservative value of ± 3 eV b for the theoretical uncertainty would lead to a very similar result of 18.7 ± 1.9 eV b).

These results are in good agreement with some of the previous direct experiments [13,20,21] (see [22] for a comment on the recoil nuclei escape in Refs. [13,20]). Concordant results but with larger uncertainties have also been reported in recent studies of the inverse process [23,24] and of transfer reactions [25].

The present result, which includes a total uncertainty significantly lower and better founded than in higher-energy measurements should help in clarifying the interpretation of solar neutrino experiments.

J. J. Correia, R. Daniel, D. Linget, and N. Karkour are gratefully acknowledged for experimental support. Valuable discussions with M. R. Haxton are greatly acknowledged. This work was supported in part by Region Aquitaine.

*Present address: GSI mbH, Planckstrasse 1, D-64291 Darmstadt, Germany.

†Permanent address: LPNHE, Ecole Polytechnique, 91128 Palaiseau, France.

[1] J. N. Bahcall *et al.,* Phys. Rev. D **58**, 096016 (1998).
[2] A. S. Brun *et al.,* Astrophys. J. **506**, 913 (1998).
[3] P. Morel *et al.,* Astron. Astrophys. **350**, 275 (1999).
[4] H. Schlattl *et al.,* Phys. Rev. D **60**, 60 (1999).
[5] F. Hammache *et al.,* Phys. Rev. Lett. **80**, 928 (1998).
[6] E. Adelberger *et al.,* Rev. Mod. Phys. **70**, 1280 (1998).
[7] G. Bogaert *et al.,* Nucl. Instrum. Methods Phys. Res., Sect. B **89**, 8 (1994).
[8] F. Hammache, thesis, 1999 (http://www-csnsm.in2p3.fr/astronuc/presentation_fr.html).
[9] M. Hussonois, 2000 (http://xxx.lpthe.jussieu.fr/abs/nucl-ex/0011014).
[10] J. P. Shapira *et al.,* Nucl. Instrum. Methods Phys. Res. **224**, 337 (1984).
[11] R. Brun *et al., GEANT* 3.16 User's Guide (CERN Program Library Office, 1993).
[12] D. Zahnow *et al.,* Z. Phys. A **351**, 229 (1995); D. Zahnow *et al.,* Z. Phys. A **359**, 211 (1997).
[13] B. W. Filippone *et al.,* Phys. Rev. Lett. **50**, 412 (1983).
[14] L. Weissman *et al.,* Nucl. Phys. **A630**, 678 (1998). Backscattered ^{8}B nuclei which decay outside the target are lost for delayed detection inducing smaller measured cross sections. For heavy elements target backing, the yield of the ^{8}B loss depends strongly on the beam energy and on the target composition and thickness. In this experiment at low energy, the target deposit was thick enough to stop most of backscattered ^{8}B nuclei resulting in very small ^{8}B loss. In the case of the experiment of Ref. [5], the corrections were determined in the same manner, taking advantage of precise knowledge of target composition due to careful RBS, (d, p), and PIXE analysis measurements performed during the course of the experiment. For details, see Ref. [8].
[15] J. F. Ziegler *et al., The Stopping and Range of Ions in Solids* (Pergamon Press, New York, 1985), Vol. 1, and the SRIM96 program.
[16] P. Descouvemont and D. Baye, Nucl. Phys. **A567**, 341 (1994).
[17] C. W. Johnson *et al.,* Astrophys. J. **392**, 320 (1992); F. M. Nunes *et al.,* Nucl. Phys. **A634**, 527 (1998).
[18] $S(0) = 19.1 \pm 1.2$ eV b is obtained when experimental values are corrected for the ^{8}B escape effect [14]. $S(0) = 18.5 \pm 1.0$ eV b was deduced from uncorrected data in Ref. [5].
[19] F. C. Barker, Nucl. Phys. **A588**, 693 (1995); A. Csoto, Phys. Lett. B **394**, 247 (1994); K. Benacceur *et al.,* J. Phys. G **24**, 1631 (1998).
[20] F. J. Vaughn *et al.,* Phys. Rev. C **2**, 1657 (1970).
[21] M. Hass *et al.,* Phys. Lett. B **462**, 237 (1999).
[22] In these measurements, escape of recoil nuclei out of the target was not corrected, and cannot be accurately calculated since the detailed compositions of the targets was not measured. However, the correction is expected to be small (less than 5%) in view of the quoted target thicknesses and taking into account of the fact that ^{8}B escape is partly counterbalanced by that of ^{8}Li in these measurements which rely on ^{7}Li$(d, p)^8$Li normalization.
[23] T. Kikuchi *et al.,* Eur. Phys. J. **A3**, 213 (1998).
[24] N. Iwasa *et al.,* Phys. Rev. Lett. **83**, 2910 (1999).
[25] A. Azhari *et al.,* Phys. Rev. Lett. **82**, 3960 (1999).